



# A Water Molecule Triggers Guest Exchange at a Mono-Zinc Centre Confined in a Biomimetic Calixarene Pocket: a Model for Understanding Ligand Stability in Zn Proteins

Emilio Brunetti,<sup>[a, d]</sup> Lionel Marcelis,<sup>[a]</sup> Fedor E. Zhurkin,<sup>[b]</sup> Michel Luhmer,<sup>[c]</sup> Ivan Jabin,<sup>[d]</sup> Olivia Reinaud,<sup>\*[b]</sup> and Kristin Bartik<sup>\*[a]</sup>

**Abstract:** In this study, the ligand exchange mechanism at a biomimetic Zn<sup>II</sup> centre, embedded in a pocket mimicking the possible constraints induced by a proteic structure, is explored. The residence time of different guest ligands (dimethylformamide, acetonitrile and ethanol) inside the cavity of a calix[6]arene-based tris(imidazole) tetrahedral zinc complex was probed using 1D EXchange Spectroscopy NMR experiments. A strong dependence of residence time on water content was observed with no exchange occurring under anhydrous conditions, even in the presence of a large excess

of guest ligand. These results advocate for an associative exchange mechanism involving the transient exo-coordination of a water molecule, giving rise to 5-coordinate Zn<sup>II</sup> intermediates, and inversion of the pyramid at the Zn<sup>II</sup> centre. Theoretical modelling by DFT confirmed that the associative mechanism is at stake. These results are particularly relevant in the context of the understanding of kinetic stability/lability in Zn proteins and highlight the key role that a single water molecule can play in catalysing ligand exchange and controlling the lability of Zn<sup>II</sup> in proteins.

## Introduction

Ligand exchange is at the basis of transition metal catalysis and has for many years been the subject of numerous studies, the essence of which is described in textbooks as following an associative or a dissociative mechanism.<sup>[1]</sup> The mechanism depends essentially on the nature and oxidation state of the metal ion, but also on its first coordination sphere and more specifically its geometry and the number and nature of the ligands that tune the ion Lewis acidity. Metal ions in an octahedral and square-base environment are the prototypes of dissociative and associative mechanisms, respectively, whereas for tetrahedral (Td) and 5-coordinate metal ions, ligand

exchange can be either dissociative or associative. Ligand exchange is also at the heart of metallo-enzyme catalysis.<sup>[2]</sup> The proteic pocket where the metal ion is located defines not only the number and nature of amino-acid residues present in the metal ion first and second coordination spheres, but also the space available for exogenous binding. This space restricts the number of accessible labile sites and is controlled by the channel giving access to the catalytic metal ion.

In the biological context, water plays a variety of key roles. It is of course the solvent, hence present in large quantity and theoretically fully available. It is, however, absent in membranes and located at very specific positions in proteins. In enzymes, it can be a reactant (in hydration and hydrolyses reactions for example), a proton provider or acceptor, especially in redox reactions, or just a relay. In metallo-enzymes more specifically, water molecules often play the role of labile ligand completing the coordination sphere of the catalytic metal ion in its resting state.<sup>[3–6]</sup> In mono-oxygenases, water plays a key role in the regulation of the catalytic activity as its dissociation is required for O<sub>2</sub> activation.<sup>[7]</sup> In the case of hydrolytic zinc enzymes, the metal is most often bound to three amino acid residues, generally histidine (His), and a water molecule completes its coordination sphere in a tetrahedral environment.<sup>[6]</sup> This water molecule can then either be activated by deprotonation, thereby giving rise to a hydroxide ion at physiological pH (such as in carbonic anhydrases),<sup>[8]</sup> activated by a hydrogen-bonded general base (e.g., in metallo-peptidases),<sup>[9]</sup> or displaced by the substrate (e.g., alcohol dehydrogenases)<sup>[10]</sup> or an inhibitor.<sup>[11]</sup> This raises questions relative to the role of water molecules in substrate binding, product release, as well as in inhibitor efficiency when the latter presents a coordinating site.

[a] Dr. E. Brunetti, Dr. L. Marcelis, Prof. K. Bartik  
Engineering of Molecular Nanosystems  
Université libre de Bruxelles  
Avenue F. D. Roosevelt 50, CP165/64, 1050 Brussels (Belgium)  
E-mail: Kristin.Bartik@ulb.be

[b] Dr. F. E. Zhurkin, Prof. O. Reinaud  
Laboratory of Pharmacological and Toxicological Chemistry and Biochemistry  
Université Paris Descartes  
45, rue des Saints-Pères, 75006 Paris (France)  
E-mail: Olivia.reinaud@parisdescartes.fr

[c] Prof. M. Luhmer  
High-Resolution Nuclear Magnetic Resonance laboratory  
Université libre de Bruxelles  
Avenue F. D. Roosevelt 50, CP165/64, 1050 Brussels (Belgium)

[d] Dr. E. Brunetti, Prof. I. Jabin  
Laboratory of Organic Chemistry  
Université libre de Bruxelles  
Avenue F. D. Roosevelt 50, CP165/64, 1050 Brussels (Belgium)

Supporting information for this article is available on the WWW under <https://doi.org/10.1002/chem.202102184>

Model complexes can help provide insight, at the molecular level, into metallo-enzyme catalysis. Of particular interest are metal complexes with a biomimetic first coordination sphere and a cavity surrounding the labile site.<sup>[12–13]</sup> With regards to the specific role of water molecules, “funnel complexes” based on calix[6]arene-based tris(imidazole) ligands<sup>[14]</sup> have provided interesting and unique information on the possible key roles of water molecules in the activity of a biomimetic metal ion (Figure 1). It has, for example, been shown that the number of water molecules embedded in the calix[6]arene funnel cavity determines the redox potential of a copper centre, shifting an irreversible system at very high potential ( $E_p^{Ox} = +0.75$  V vs. Fc) in the absence of water, to a very low potential ( $E_p^{Red} = -0.35$  V) when a single molecule of water is bound in the cavity, and to a fully reversible state ( $E^{o'} = 0.13$  V) when two molecules fill the cavity.<sup>[15]</sup> This highlights that water molecules are able to control the redox activity of a biomimetic metal centre.

Two types of aqua-metal complexes have been reported with the calix[6]arene-based tris(imidazole) system. The first type of complexes has a water molecule coordinated to the metal centre in the endo position, inside the cavity. When the calixarene presents six *t*Bu groups at its large rim, as in the case of ligand 1' (Figure 1b), it has been shown with a  $Zn^{II}$  complex that a second water molecule, H-bonded to the first one, is also embedded in the cavity thus optimizing its filling.<sup>[16–18]</sup> The second type of complexes are those with a water molecule bound in the exo position, when an organic guest ligand sits

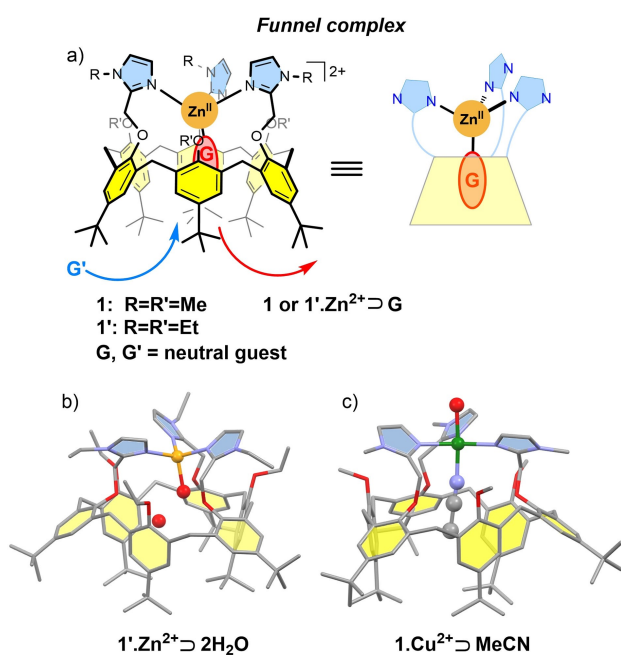


**Figure 1.** Supramolecular biomimetic systems obtained with calix[6]arene-based tris(imidazole) funnel metal complexes: a) molecular and schematized representation of the  $Zn^{II}$  complexes obtained with the calix[6]-tris(imidazole) ligands 1 or 1'; b) XRD structures of the aqua- $Zn^{II}$  complex  $1'.Zn^{2+} \supset 2H_2O$ , model for the active site of carbonic anhydrase, with water molecules represented as a red sphere;<sup>[17]</sup> c) XRD structures of the  $Cu^{II}$  acetonitrile complex  $1.Cu^{2+} \supset MeCN$  presenting a water ligand (red sphere) selectively bound in the exo-position.<sup>[20]</sup>

selectively in the endo position. This leads to a 5-coordinate metal centre, as observed with  $Cu^{II}$  complexes based on ligand 1 (Figure 1c).<sup>[19]</sup> In all cases, the endo-bound molecules can be selectively exchanged for a variety of organic guest ligands.

We are interested in the mechanism of guest exchange within the biomimetic calix[6]-tris(imidazole) cavity (Figure 1a). With 5-coordinate  $Cu^{II}$  complexes and 4-coordinate  $Cu^I$  complexes we have shown that guest ligand exchange is dissociative proceeding through 3- and 4-coordinate intermediates, respectively, with empty cavities.<sup>[20]</sup> While, the thermodynamics of guest ligand exchange with tetrahedral  $Zn^{II}$  complexes has been studied in detail,<sup>[21]</sup> fundamental questions remain unanswered regarding the exchange mechanism. The objective of the study reported here is to decipher the mechanism of guest ligand exchange at the level of biomimetic 4-coordinate  $Zn^{II}$  centres, and the possible role of water molecules in the mechanism. To do this, the residence time of three different guests ( $G =$  dimethylformamide, acetonitrile and ethanol) inside the calixarene cavity of the biomimetic calix[6]-tris(imidazole) was probed, under different conditions, using 1D EXSY (EXchange Spectroscopy) NMR experiments.<sup>[22]</sup> Theoretical modelling was also undertaken.

## Results and Discussion

### Possible guest exchange mechanisms

Theoretically, three mechanisms can be envisaged for guest-exchange with calix[6]arene- $Zn^{II}$  complexes based on ligand 1 (complex A,  $1.Zn^{2+} \supset G$ , Figure 2):

- The associative endo-exchange mechanism (Figure 2, path a), with the threading in of a new guest molecule and in situ replacement of a guest already present. Such a mechanism, at work in classical Td  $Zn^{II}$  complexes devoid of cavity constrains, can however be ruled out because of the shape of the cavity; the size of the small rim that surrounds the labile metal coordination site impedes the simultaneous coordination of an incoming and an outgoing guest (as in intermediate B).
- The dissociative mechanism (Figure 2, path b), where the guest trapped inside the calixarene cavity leaves the cavity, thus enabling a new guest to enter. Such a mechanism appears, a priori, highly unfavorable as it leads to the transient formation of a 3-coordinate dicationic complex (intermediate C), which is a rare if not unknown species due to the high Lewis acidity of  $Zn^{II}$  in such an electronically poor environment.
- The associative exo-assisted exchange mechanism (Figure 2, path c). The first step in this case is the exo-coordination of a ligand L at the level of the zinc dication, which gives rise to a 5-coordinate  $Zn^{II}$  centre with a trigonal bipyramidal (Tbp) geometry (intermediate D). The endo-coordinated guest then leaves the calixarene cavity (4-coordinate intermediate E), thus enabling the endo-coordination of a new guest. The subsequent decoordination of the exo-ligand restores the starting tetrahedral geometry. The exo-ligand L could be the solvent, or even the guest itself, but water is of course also a likely candidate.

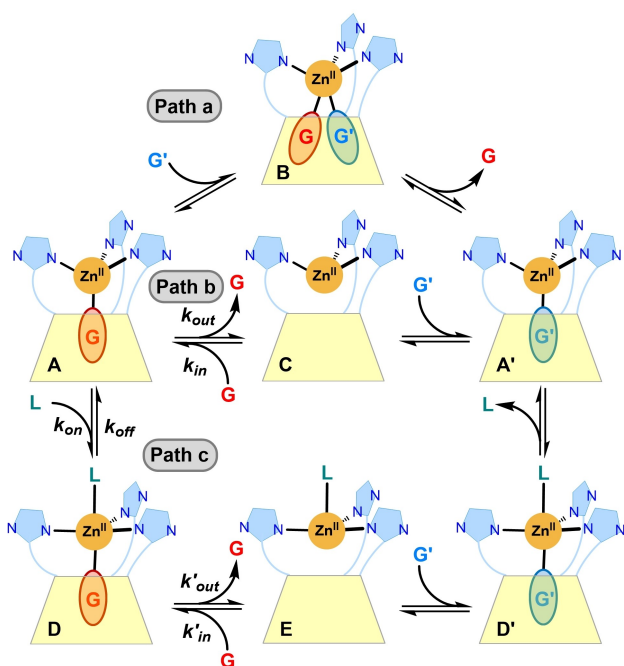
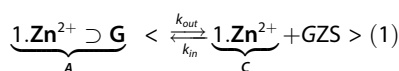


**Figure 2.** Possible mechanisms for guest exchange within host  $1.Zn^{2+} \supset G$ . Path a: associative endo-exchange mechanism; path b: dissociative exchange mechanism with a 3-coordinated intermediate state; path c: associative exo-assisted exchange mechanism with 5- and 4-coordinate intermediate states.

### Kinetic models for the dissociative and exo-assisted exchange mechanisms

If only the dissociative exchange mechanism (Figure 2, path b) takes place, the release of an encapsulated guest is described by the equilibrium between the host-guest complex and the empty calixarene host [Eq. (1)]. The inverse of the residence time  $\tau_G^{-1}$  of the guest inside the calixarene cavity is then given by Equation (2).<sup>[23]</sup>



$$\tau_G^{-1} = k_{out} \quad (2)$$

With the associative exo-assisted exchange mechanism (Figure 2, path c), two equilibria must be considered: the equilibrium between the host-guest complex and the complex with an exo-coordinated ligand [Eq. (3)] and the equilibrium between the latter and the exo-coordinated empty host [Eq. (4)]. The inverse of the residence time of the guest inside the calixarene cavity [Eq. (5)] depends consequently not only on the kinetic constant that describes the release of guest G from the exo-coordinated intermediate,  $k'_{out}$ , but also on the affinity constant  $K_1$  ( $= k_{on}/k_{off}$ ), that characterizes the affinity of the host-guest complex for the exo ligand L.<sup>[23]</sup>



$$\tau_G^{-1} = \frac{k'_{out} K_1 [L]}{1 + K_1 [L]} \quad (5)$$

Should both mechanisms take place, the inverse of the residence time in the cavity will then be given by Equation (6).<sup>[23]</sup>

$$\tau_G^{-1} = \frac{k_{out} + k'_{out} K_1 [L]}{1 + K_1 [L]} \quad (6)$$

By measuring the residence time of the guest in the cavity as a function of [L] (the concentration of potential exo-ligand), it should thus be possible to determine if the proposed exo-assisted exchange mechanism is at stake. Residence times can be determined using 1D NMR EXSY experiments, which were undertaken with three different guests: DMF, MeCN and EtOH.

### <sup>1</sup>H NMR characterization of the host-guest Zn<sup>II</sup> complexes of the calix[6]-tris(imidazole)

The DMF, MeCN and EtOH adducts of calix[6]-tris(imidazole),  $1.Zn^{2+} \supset G$ , can be readily generated in a non-coordinating solvent by solubilizing the aqua Zn<sup>II</sup> complex  $1.Zn^{2+} \supset (H_2O)_2$  in the presence of the coordinating guest that replaces the two water molecules present inside the calix[6]arene cavity. The <sup>1</sup>H NMR spectra of these host-guest complexes, recorded in CD<sub>2</sub>Cl<sub>2</sub> at 298 K, are displayed in Figure 3.<sup>[23]</sup> As previously observed in CDCl<sub>3</sub>,<sup>[21]</sup> these complexes present a <sup>1</sup>H NMR signature characteristic of a C<sub>3v</sub> symmetrical calix[6]arene-based species adopting a major flattened conformation ( $\Delta\delta_{tBu}$  and  $\Delta\delta_{ArH} > 0.5$  ppm). The simultaneous presence of up-field shifted signals (<0.5 ppm), characteristic of the guest embedded in the cavity, and of signals for the free ligand indicates a slow exchange regime relative to the NMR chemical shift time scale. In the case of the EtOH adduct, the signal of the included guest is broadened at RT and narrows down when decreasing temperature,<sup>[23]</sup> indicating that in this case guest exchange is not infinitely slow at RT.

The binding affinities for ethanol and acetonitrile relative to dimethylformamide were determined via competitive <sup>1</sup>H NMR titration experiments:  $K_{EtOH/DMF}$  (298 K) =  $0.7 \pm 0.1$  and  $K_{MeCN/DMF}$  (298 K) =  $0.21 \pm 0.03$ .<sup>[24]</sup>

### 1D EXSY experiments with MeCN and DMF

As guest exchange is slow on the chemical shift timescale, the residence time of the guest molecules in host  $1.Zn^{2+}$  can be determined by selective inversion 1D EXSY experiments. These experiments yield more reliable results than line-shape analysis

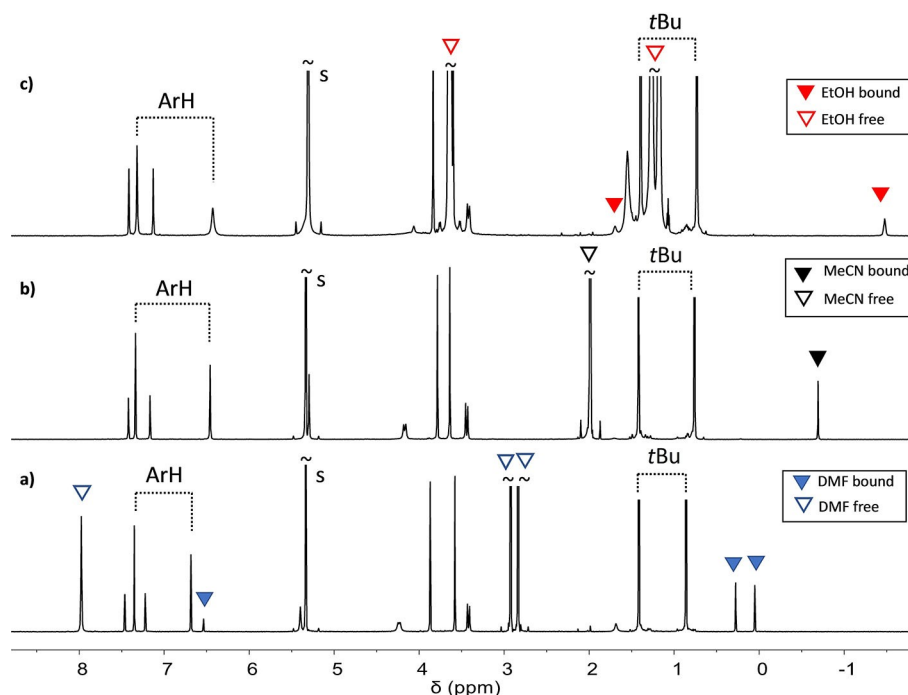


**Figure 3.**  $^1\text{H}$  NMR spectra (600 MHz) of  $1.\text{Zn}^{2+}\cdot\text{Guest}$  in  $\text{CD}_2\text{Cl}_2$  under low water content (less than 10 equiv. water) at 298 K (a)  $[1.\text{Zn}^{2+}] = 8.7 \times 10^{-4}$  M; 32 equiv. DMF; (b)  $[1.\text{Zn}^{2+}] = 1.46 \times 10^{-3}$  M; 42 equiv. MeCN; (c)  $[1.\text{Zn}^{2+}] = 1.24 \times 10^{-3}$  M; 120 equiv. EtOH. s: solvent.

and have already been used to study several supramolecular host-guest complexes, including calixarene-based systems.<sup>[25]</sup> Selective excitation at the frequency of a signal of the included guest in the high-field region of the spectrum was performed.

Experiments to evaluate the possible role of water in the exchange mechanism were carried out first with the non-protic guests MeCN and DMF.<sup>[23]</sup> Considering that water is a competitor for the calixarene cavity, all experiments were undertaken with a large excess of guest (i.e., 32 equiv. DMF, 42 equiv. MeCN) to ensure that even at the higher water concentrations all cavities are filled with the guest. Starting with near anhydrous host-guest solutions, various quantities of water were added to the NMR tube. Water concentration was determined via signal integration (relative to the signals of the host of known concentration). The inverse of the residence times of the guests was determined as a function of water concentration and the results are reported in Figure 4, clearly showing a strong dependence of the residence time of the guest on water content.

The NMR spectra of the two systems did not change upon the addition of water (except for the water signal) hence suggesting that the 4-coordinate host-guest complex remains the only detectable species. Considering this and the water concentrations used for the experiments, the product  $K_1[\text{L}]$  in Equation (6) can be considered negligible compared to 1. Equation (6) can thus be reduced to the linear expression given by Equation (7):

$$\tau_G^{-1} = k_{out} + k'_{out} K_1[\text{L}] \quad (7)$$

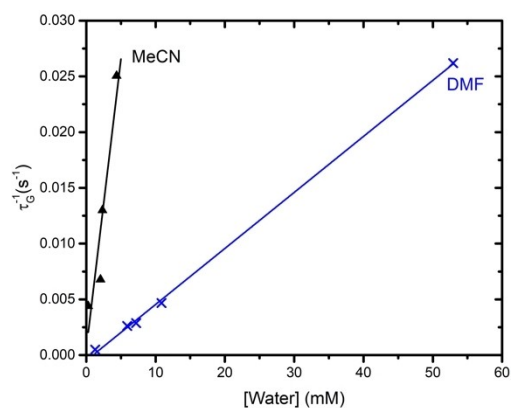


**Figure 4.** Dependence of the inverse of the residence time ( $\tau_G^{-1}$ ) of MeCN ( $[1.\text{Zn}^{2+}] = 1.24$  mM, 42 equiv. MeCN), and DMF ( $[1.\text{Zn}^{2+}] = 0.87$  mM, 32 equiv. DMF) as a function of water concentration, derived from 1D EXSY experiments undertaken at 298 K in  $\text{CD}_2\text{Cl}_2$ .<sup>[23]</sup> Fitting (solid lines) according to Equation (7) ( $\text{L} = \text{H}_2\text{O}$ ).

Equation (7) was fitted to the variation of the inverse of the residence time of the included guest as a function of water concentration (Figure 4). The fitting yields a slope ( $k'_{out}K_1$ ) which is one order of magnitude smaller when DMF is the guest, compared to MeCN ( $0.50 \pm 0.05$  and  $5.2 \pm 0.5$   $\text{s}^{-1}\text{M}^{-1}$ , respectively). Extrapolation to pure anhydrous conditions suggests that little, or no, exchange occurs in the total absence of water for both guests. It is however quantitatively difficult to determine the water concentration and the residence time under such conditions, and the dissociative mechanism cannot be formally ruled out but, if present, it is clearly negligible ( $k_{out}$

$\approx 0 \text{ s}^{-1}$ ). The results advocate that the associative exchange mechanism implicating the transient exo-coordination of water is at stake both with DMF and MeCN. As all experiments were undertaken with a large excess of guest, to ensure that all cavities are always filled with the guest, and as negligible exchange was observed in the absence of water, these guests clearly do not play the role of exo-ligand. A hypothesis that can be put forward is that they are sterically too hindered to interact with the zinc centre at the level of the imidazole moieties via exo-coordination.

The thermodynamic and kinetic data obtained deserve some further comments. The relative affinity  $K_{\text{MeCN/DMF}}(298 \text{ K}) = 0.21$  indicates that DMF is more strongly bound to the  $\text{Zn}^{\text{II}}$  centre than MeCN, in accordance with its higher Lewis donor ability. This advocates for a more enthalpically costing metal-guest bond cleavage, and thus a smaller  $k'_{\text{out}}$  value. Indeed, the stronger the metal to ligand bond, the slower the dissociation step. DMF, as the best donor guest, also makes the  $\text{Zn}^{\text{II}}$  centre less Lewis acidic, and consequently, the coordination of a fifth ligand, namely here water, less enthalpically favorable. Consequently, the  $K_1$  value is probably smaller for DMF than for MeCN. The  $k'_{\text{out}}K_1$  product for DMF is thus expected to be smaller than for MeCN, which is consistent with the EXSY measurements. This also suggests that the rate determining step for ligand exchange lies somewhere in between intermediates D and E (Figure 2, path c).

### 1D EXSY experiments with the protic guest EtOH

The signals of the encapsulated EtOH at 298 K are broad, qualitatively indicating that the rate of guest exchange is faster with EtOH than with DMF and MeCN at this temperature. EXSY NMR experiments with various water concentrations were carried out with EtOH at 253 K.<sup>[23]</sup> It is clear that the linewidth of the methyl signal of the encapsulated guest (at  $\sim -1.55 \text{ ppm}$ ) is sensitive to water concentration (Figure 5a), further proof of the effect of water concentration on the exchange kinetics. As

observed with MeCN and DMF, the inverse of the residence time of EtOH in host  $1.\text{Zn}^{2+}$  increases with water concentration and is negligible at low water concentration (Figure 5b). Compared to the two other guests the observed variation is clearly not linear, but it is consistently at least one order of magnitude larger (e.g., the inverse of the residence time for  $[\text{H}_2\text{O}] = 5 \text{ mM}$  is around  $0.2 \text{ s}^{-1}$  for EtOH,  $0.025 \text{ s}^{-1}$  for MeCN and  $0.002 \text{ s}^{-1}$  for DMF).

Interestingly, when more EtOH was added to the solution containing ca. 14 mM water, a significant decrease of the exchange kinetics was observed (by a factor of approximately 4, Figure 5b). The explanation that can be put forward to explain the non-linearity and the decrease in the kinetics upon EtOH addition, is that in dichloromethane, which is a relatively apolar solvent, EtOH will interact with the water molecules, which are consequently less prone to coordinate the metal centre and act as catalyst for the guest exchange. The effect of the concentration of EtOH on the exchange process at constant water concentration was also scrutinized. A systematic decrease of the exchange kinetics was observed with increasing EtOH concentration (Figure 5c).<sup>[26]</sup> This clearly also confirms that EtOH does not play the role of exo-ligand leading to exchange catalysis.

### Computer modelling studies

The mechanism for guest exchange was further explored through theoretical modelling, with MeCN as guest. The dissociative and associative mechanisms (Figure 2, paths b and c) were scrutinized by DFT modelling using the BP86-D3 calculation method.<sup>[23]</sup> For simplicity, the alkyl groups of the imidazole moieties were replaced by hydrogen atoms.

In the associative pathway (Figure 6, right) the exo-coordination of a water molecule leads to the formation of a 5-coordinate trigonal bipyramidal  $\text{Zn}^{\text{II}}$  intermediate (D) that exhibits some distortion along the z axis. This intermediate has an energy which is only +24 kJ/mol above that of the starting tetrahedral complex (A).<sup>[27]</sup> The second step leads to a new 4-

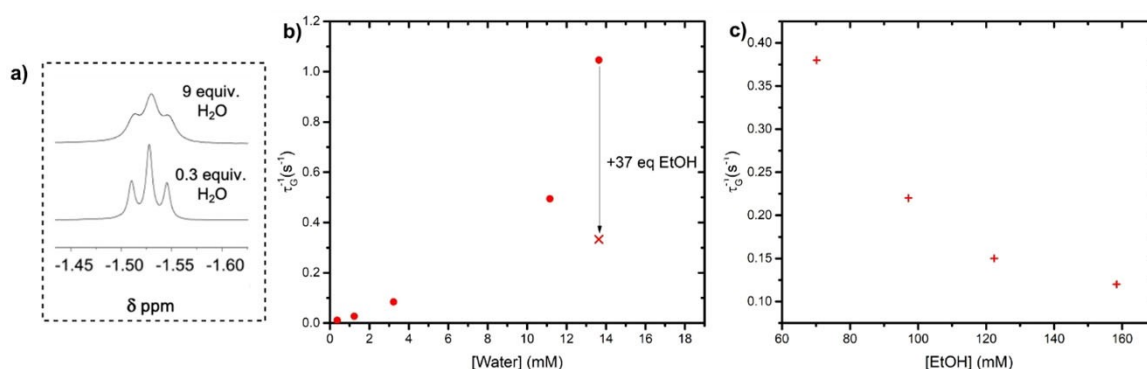


**Figure 5.** a)  $^1\text{H}$  NMR signal of the included guest methyl group of  $1.\text{Zn}^{2+}\cdot\text{EtOH}$  in  $\text{CD}_2\text{Cl}_2$  at 253 K (600 MHz,  $[1.\text{Zn}^{2+}] = 1.24 \text{ mM}$ , 53 equiv. EtOH), in the presence of (bottom) 0.3 equiv. of water and (top) 9 equiv. of water; b) Corresponding dependence of the inverse of the residence time ( $\tau_G^{-1}$ ) of EtOH as a function of water concentration.<sup>[23]</sup> The cross depicts the evolution of the kinetic of exchange of EtOH upon addition of an extra 37 equiv. EtOH; c) Inverse of the residence time ( $\tau_G^{-1}$ ) of EtOH in the host cavity at 253 K as a function of EtOH concentration ( $[1.\text{Zn}^{2+}] = 1.8 \text{ mM}$ ,  $13 \pm 1 \text{ equiv. H}_2\text{O}$ ,  $\text{CDCl}_3$ ).<sup>[23]</sup>

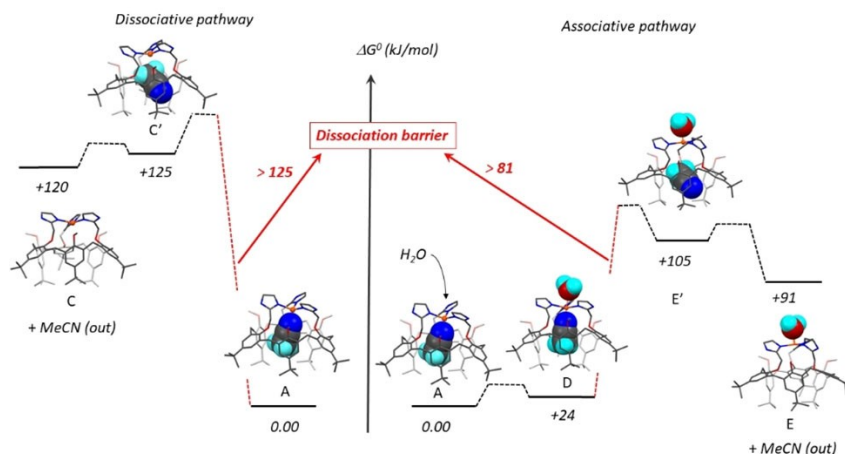


**Figure 6.** Comparison of the two pathways energetics in dichloromethane (BP86-D3, SMD solvation model).<sup>[23]</sup> Free energy (in kJ/mol) is calculated with respect to 1 M standard state. See Figure 2 for naming of the different species involved in both pathways.

coordinate species ( $E'$ ), where the coordination link between the acetonitrile donor and  $Zn^{II}$  is broken. The MeCN guest remains included in the calixarene cavity but reorients itself with the N atom no longer oriented towards the metal ion. In this high-energy intermediate (+81 kJ/mol above the previous intermediate),  $Zn^{II}$  sits in a flattened tetrahedral geometry due to steric constraints imposed by the bonds to the imidazole groups of the calixarene structure. The empty cavity species is obtained in the next step, leading to the intermediate (E) with an energy 14 kJ/mol below the energy of the host/guest intermediate  $E'$ . This energy profile suggests that the transition state is close to the high-energy intermediate  $E'$  located between the penta-coordinated system, with the endo-complexed guest and exo-complexed water molecule, and the tetracoordinated system E with the empty cavity and exo-coordinated water molecule. Various trials to find its exact positioning were unsuccessful, which is probably due to the flatness of the potential energy surface around intermediates  $E'$  and E. It is noteworthy that intermediate host-guest complexes devoid of a coordination bond to the cavity guest have been experimentally detected, by low-temperature  $^1H$  NMR studies of nitrilo ligand exchange in calix[6]-based copper(I) complexes; no information on their exact structure was however obtained.<sup>[28]</sup>

In the dissociative pathway (Figure 6, left), the initial step consists in the cleavage of the bond between the MeCN guest and  $Zn^{II}$ , leading to a three-coordinate intermediate  $C'$ , where  $Zn^{II}$  sits in a distorted trigonal planar environment. Interestingly, in this intermediate, as in the associative pathway (structure  $E'$ ), the MeCN molecule is still embedded in the cavity with an “upside down” orientation. Expulsion of the MeCN guest in the second step, leads to the empty cavity intermediate C, which is of similar energy. As previously, the exact positioning of the transition state could not be found but intermediate  $C'$ , which is the one with the highest energy, should be a good approximation. Thus, the overall activation energy of the dissociative pathway should be no less than 125 kJ/mol,

compared to 105 kJ/mol for the associative pathway, the latter value including an overestimated water molecule solvation energy.<sup>[27]</sup> A more remarkable difference is observed when comparing the dissociation barriers of the tetrahedral complex (>125 kJ/mol) and aqua-trigonal-bipyramidal complex (>81 kJ/mol). This significant difference is a consequence of the relative stabilities of corresponding dissociation products. Indeed, the overall free energy cost of the expulsion of acetonitrile in the dissociative pathway leading to the trigonal product C (from the initial 4-coordinate compound A) is 120 kJ/mol, whereas it is only 66 kJ/mol in the associative pathway (starting from the 5-coordinate D) leading to the inverted tetrahedral (aqua) $Zn$  complex E. This large activation energy difference highlights an impressive difference in the lability of the  $Zn^{II}$  ligands when in a 4- or 5-coordinated system.

The unexpected existence of intermediates  $C'$  et  $E'$  indicates that the opening of the *t*Bu door has a significant energy cost, as it was experimentally evidenced with  $Cu^I$  funnel complexes. The fact that the orientation of MeCN is inverted in these intermediates may be related to this opening process, with the smaller CN group of the MeCN guest offering favourable CH- $\pi$  interactions with the *t*Bu door. Another interesting information is provided by the related modification of the geometry at the  $Zn^{II}$  centre. It remains slightly pyramidal with an endo orientation of the pyramid for the tricoordinate intermediates (C and  $C'$ ). In contrast, the pyramid is inverted, although very flat, for intermediates E and  $E'$ , to enable the exo-coordination of water. These distortions are indicative of steric constraints induced by the calixarene core, which becomes more flattened than initially. This geometry change at the  $Zn^{II}$  centre projects the *t*Bu groups towards each other, a phenomenon which is stronger when the pyramid is inverted such as in E and  $E'$ , in agreement with the higher energy release from  $E'$  to E, compared to  $C'$  to C.

From these modelling studies, we can confidently propose that the dissociative mechanism leading to 3-coordinate intermediates is highly unlikely, being much more energy

demanding compared to the associative one that leads to more stable 5-coordinate intermediates.

In order to further validate the computational model, a variable temperature study was undertaken with  $1 \cdot \text{Zn}^{2+} \supset \text{MeCN}$ . EXSY data were recorded in the 308 to 288 K temperature range and an Eyring-type regression was applied to the measured rate constants.<sup>[23]</sup> This regression yields values for the difference in enthalpy ( $26 \pm 2$  kJ/mol) and entropy ( $-125 \pm 8$  J/mol.K) between species A and E' (Figure 6). The highly negative entropy value is in full agreement with the proposed transition state that involves the flip of the embedded acetonitrile guest in the ternary adduct (CalixZn/MeCN/H<sub>2</sub>O). The positive enthalpy value substantiates a rate determining step implying cleavage of the metal-guest bond (Zn-MeCN). The corresponding difference in free energy at 298 K ( $63 \pm 3$  kJ/mol) is somewhat smaller than the computed value but this can be rationalized by the fact that the solvation energy of a free water molecule is largely overestimated in the computational model.<sup>[23]</sup>

## Discussion and Conclusion

Although ligand-exchange in  $\text{Zn}^{\text{II}}$  complexes has been the subject of many studies,<sup>[29]</sup> often in water, little has been reported for tetrahedral dicationic complexes. The main reason stems from their scarcity. Indeed, in a 4-coordinate environment with only neutral ligands, the  $\text{Zn}^{\text{II}}$  metal centre displays strong Lewis acidity and residual water present in the solvent classically ionizes to give rise to monocationic hydroxo complexes, which, in turn, readily undergo dimerization. The Td, dicationic aqua  $\text{Zn}^{\text{II}}$  complex based on the tris(imidazole) core of ligand **1** was, when published, the first of its kind.<sup>[16]</sup> Intriguingly, such a Td neutral donor environment is common in Zn enzymes because the proteic pocket isolates the mononuclear centre, preventing its dimerization, and provides a stabilizing second coordination sphere. With the biomimetic Funnel  $\text{Zn}^{\text{II}}$  complex based on **1**, the calixarene structure not only controls the second coordination sphere, with H-bond acceptors in the vicinity of the endo-coordination site (occupied by the guest-ligand), but also a cavity space that restricts access to the metal centre (although open to the solvent) and precludes simultaneous coordination of two guest ligands in the endo position. Yet, guest ligand occurs, the mechanism of which was to date unclear.

The studies herein reported have unambiguously shown that:

- (i) A dissociative guest ligand exchange mechanism that would give rise to a 3-coordinate dicationic complex as an intermediate is not operating.
- (ii) Guest ligand exchange occurs through an associative mechanism that involves double exchange and inversion of the pyramid at the  $\text{Zn}^{\text{II}}$  centre.
- (iii) A single water molecule plays the role of a catalyst by transiently coordinating the  $\text{Zn}^{\text{II}}$  centre in the exo position, trans to the guest-ligand, thereby allowing the guest-ligand to leave the cavity.

- (iv) Among the tested molecules (water, a nitrile, an alcohol and an amide), only a water molecule appears to be able to play this role of catalyst.
- (v) The activity of the water molecule is modulated by its environment, being more or less available as a ligand in the presence/absence of H-bond donors or acceptors (e.g., EtOH).

The water molecule plays, in the system studied, a role similar to that of a hemi labile ligand in the previously reported calix[6]-based funnel complexes capped by a phenol group.<sup>[30]</sup> Most interestingly, a mechanism involving a hemi labile ligand and double displacement and inversion of the pyramid at a Td  $\text{Zn}^{\text{II}}$  centre has been proposed for substrate binding and product release in some enzymes. In Horse Liver Alcohol Dehydrogenase,<sup>[31]</sup> it has, for example, been shown that a glutamate residue (Figure 7) participates in a double-displacement interchange mechanism, via a trigonal bipyramidal geometry. The residue displaces, in a first step, the water molecule bound to the metal ion, and in a second step, the substrate oxygen (an alcohol) displaces the glutamate residue to give rise to the structure observed in the ternary complexes (enzyme/cofactor NAD<sup>+</sup>/alcohol substrate). The water dissociates from the enzyme through the hydrophobic substrate binding barrel, and the substrate then enters the channel and binds to the zinc ion. Similarly, the active-site zinc in human glutathione-dependent formaldehyde dehydrogenase undergoes coenzyme-induced displacement and transient coordination to a highly conserved glutamate residue during the catalytic cycle.<sup>[32]</sup> The glutamate residue in these enzymes plays the same role as the water molecule in our system.

The fact that the  $\text{Zn}^{\text{II}}$  ion in such a Td constrained environment becomes totally inert in the absence of a catalytic donor (the smallest being a water molecule) may well explain different important phenomena observed in Zn proteins such as the high kinetic stability of Td Zn sites, in Zn fingers, but also of enzymes such as carbonic anhydrase.<sup>[33]</sup> It may also be of relevance in the destabilization of  $\text{M}^{\text{II}}$  binding to proteins when a ligand or a mutation leads to small structural changes around the metal binding site that can open access to water. Hence, the very high energy of trigonal  $\text{Zn}^{\text{II}}$  complexes and the consequent requirement of a ligand associative assistance for ligand exchange, the role of which can be played by a water molecule, probably also plays a key role in for trafficking, transport, and reactivity of Zn in cells.<sup>[6,34–35]</sup>

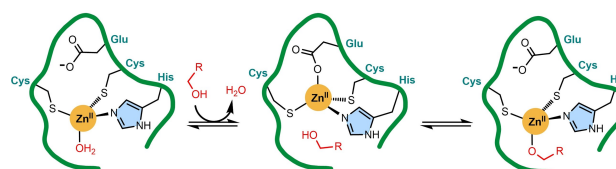


**Figure 7.** Schematic representation of the double displacement, interchange mechanism for substrate binding/product release proposed for horse liver alcohol dehydrogenase.<sup>[31]</sup>

## Experimental Section

**General experimental methods:**  $^1\text{H}$  NMR spectra were recorded on a Varian 600 MHz spectrometer. 2D NMR spectra (COSY, HSQC and ROESY) were recorded to complete signal assignments. NMR parameters (acquisition time, recycling times, and signal accumulation) were chosen to ensure that quantitative data could be obtained from signal integration in the 1D  $^1\text{H}$  spectra. The exact concentration of the receptor in the different solutions was determined using an external reference of known concentration. Concentrations of guest and water were determined by signal integration relative to the host signals. The near anhydrous conditions were obtained by adding molecular sieves into the NMR tubes. Traces of residual solvent were used as an internal chemical shift reference. Chemical shifts were quoted on the  $\delta$  scale. Calixarene 1 was synthesized as described in the literature.<sup>[21]</sup>

**Determination of the relative affinity of Guest 1 compared to Guest 2 in DCM-d<sub>2</sub> via  $^1\text{H}$  NMR competitive binding studies:** A known amount of equivalents of Guest 1 and Guest 2 were added in 600  $\mu\text{L}$  of a  $\text{CD}_2\text{Cl}_2$  solution of complex  $1.\text{Zn}^{2+}$ . Distinct signals were observed for both the complexes and for the free guests, indicating slow exchange on the chemical shift time scale. The integrations of the signals corresponding to free guests and the included guests were used to calculate relative affinity defined as  $[\text{Guest}2_{\text{in}}]/[\text{Guest}1_{\text{in}}] \times [\text{Guest}1_{\text{Free}}]/[\text{Guest}2_{\text{Free}}]$  (errors estimated  $\pm 20\%$ ).

**1D EXSY NMR experiments:** 1D EXSY experiments were recorded using a gradient-selected (DPFGSE) sequence with iburp2 shaped pulses with selective excitation applied at the frequency of a signal of the guest buried inside the calixarene cavity. The evolution with mixing time  $\tau_m$  of the normalized integrated intensity of the signals of the bound and free guests was monitored. The integrated intensities at equilibrium,  $\text{lin}^\circ$  and  $\text{lout}^\circ$ , were measured in a spectrum obtained with a single  $90^\circ$  pulse recorded with identical receiver gain (generally 32 transients with acquisition time and relaxation delay tailored for each system). The pseudo first order rate constants characterizing the exchange between coordinated and free guest were determined as the initial slope of the signal intensity ratio  $(\text{lout}/\text{lin})/(\text{lout}^\circ/\text{lin}^\circ)$  as a function of mixing time.

Computational modelling was performed using RI-DFT (BP86 functional<sup>[36]</sup> with D3BJ dispersion correction<sup>[37]</sup>) as implemented in Orca v.4.2.1 software.<sup>[38]</sup> For geometry optimization and frequency calculations, def2-SVP basis set was used on C, H, O and N atoms and def2-TZVP on Zn.<sup>[39]</sup> Final electronic energies were calculated using def2-TZVP basis set on all atoms and SMD<sup>[40]</sup> solvation model with dichloromethane as solvent. Structures of dissociation intermediates were obtained from PES scan and optimized using the same model as described above.

## Acknowledgements

E.B. received a PhD grant from the *Fonds pour la formation à la Recherche dans l'Industrie et dans l'Agriculture* (FRIA-FRS, Belgium). L.M. thanks the Université libre de Bruxelles and the Wiener-Anspach Foundation for financial support. Published with the support of the *Fondation Universitaire de Belgique*.

## Conflict of Interest

The authors declare no conflict of interest.

**Keywords:** biomimetism · calixarenes · DFT modelling · funnel complexes · NMR spectroscopy

- [1] a) R. G. Wilkins, *Kinetics and mechanism of reactions of transition metal complexes*, VCH, 1991; b) J. D. Atwood, *Inorganic and organometallic reaction mechanisms*, VCH, 1997; c) R. H. Crabtree, *The Organometallic Chemistry of the Transition Metal Ions*, Wiley, 2001.
- [2] J. J. R. Frausto da Silva, R. J. P. Williams, *The biological chemistry of the elements*, Oxford Univ. Press, 2001.
- [3] I. Bertini, H. B. Gray, E. I. Stiefel, J. S. Valentine, *Biological Inorganic Chemistry, Structure and Reactivity*, University Science Books, 2007.
- [4] Special issues on Bio-inorganic Enzymology: a) *Chem. Rev.* 1996, 96, 2237–3042; b) *Chem. Rev.* 2014, 114, 3367–4038.
- [5] Special issue on Biomimetic Inorganic Chemistry: *Chem. Rev.* 2004, 104, 347–1200.
- [6] a) W. N. Lipscomb, N. Sträter, *Chem. Rev.* 1996, 96, 2375–2433; b) W. Maret, Y. Li, *Chem. Rev.* 2009, 109, 4682–4707; c) A. Krezel, W. Maret, *Arch. Biochem. Biophys.* 2016, 611, 3–19.
- [7] I. G. Denisov, T. M. Makris, S. G. Sligar, I. Schlichting, *Chem. Rev.* 2005, 105, 2253–2277.
- [8] V. M. Krishnamurthy, G. K. Kaufman, A. R. Urbach, I. Gitlin, K. L. Gudiksen, D. B. Weibel, G. M. Whitesides, *Chem. Rev.* 2008, 108, 946–1051.
- [9] N. Cerda-Costa, F. Xavier Gomis-Rüth, *Protein Sci.* 2014, 23, 123–144.
- [10] B. V. Plapp, B. Raj Savarimuthu, D. J. Ferraro, J. K. Rubach, E. N. Brown, S. Ramaswamy, *Biochem.* 2017, 56, 3632–3646.
- [11] See for example: C. Rouanet-Mehouas, B. Czarny, F. Beau, E. Cassar-Lajeunesse, E. A. Stura, V. Dive, L. Devel, *J. Med. Chem.* 2017, 60, 403–414.
- [12] Review on metallated cavities: R. Gramage-Doria, D. Armspach, D. Matt, *Coord. Chem. Rev.* 2013, 257, 776–816.
- [13] a) J.-N. Rebilly, B. Colasson, O. Bistri, D. Over, O. Reinaud, *Chem. Soc. Rev.* 2015, 44, 467–489; b) D. Coquière, S. Le Gac, U. Darbost, O. Sénèque, I. Jabin, O. Reinaud, *Org. Biomol. Chem.* 2009, 7, 2485–2500.
- [14] N. Le Poul, Y. Le Mest, I. Jabin, O. Reinaud, *Acc. Chem. Res.* 2015, 48, 2097–2106.
- [15] N. Le Poul, B. Colasson, G. Thiabaud, D. Jeanne Dit Fouque, C. Iacobucci, A. Memboeuf, B. Douziech, J. Řezáč, T. Prangé, A. de la Lande, O. Reinaud, Y. Le Mest, *Chem. Sci.* 2018, 9, 8282–8290.
- [16] O. Sénèque, M.-N. Rager, M. Giorgi, O. Reinaud, *J. Am. Chem. Soc.* 2001, 123, 8442–8443.
- [17] The presence of this second water guest depends on the substitution pattern at the large rim of the calix[6]arene. When three *t*Bu groups are replaced by three smaller  $\text{NH}_2$  groups the aromatic units can be partially embedded into the cavity that adapts to the size of a single water molecule, and the second water molecule is absent. See: D. Coquière, J. Marrot, O. Reinaud, *Org. Biomol. Chem.* 2008, 6, 3930–3934.
- [18] Inverting the design of the system, i.e., grafting the metal ion coordination site at the large rim of the calix[6]arene, instead of the small rim, showed the endo complexation of 3 H-bonded water molecules, among which only one is coordinated. See: S. Zahim, L. A. Wickramasinghe, G. Evano, I. Jabin, R. R. Schrock, P. Müller, *Org. Lett.* 2016, 18, 1570–1573.
- [19] L. Le Clainche, M. Giorgi, O. Reinaud, *Inorg. Chem.* 2000, 39, 3436–3437.
- [20] a) Y. Rondelez, M.-N. Rager, A. Duprat, O. Reinaud, *J. Am. Chem. Soc.* 2002, 124, 1334–1340; b) N. Le Poul, B. Douziech, J. Zeitouny, G. Thiabaud, H. Colas, F. Conan, N. Cosquer, I. Jabin, C. Lagrost, P. Hapiot, O. Reinaud, Y. Le Mest, *J. Am. Chem. Soc.* 2009, 131, 17800–17807.
- [21] O. Sénèque, M.-N. Rager, M. Giorgi, O. Reinaud, *J. Am. Chem. Soc.* 2000, 122, 6183–6189.
- [22] a) T. Claridge, *High-Resolution NMR techniques in organic chemistry*, Tetrahedron organic chemistry series Volume 19, Wiley, 1999; b) C. L. Perrin, T. J. Dwyer, *Chem. Rev.* 1990, 90, 935–967; c) H. Hu, K. Krishnamurthy, *J. Magn. Reson.* 2006, 182, 173–177; d) J. T. Gerig, *J. Org. Chem.* 2003, 68, 5244–5248.
- [23] See the Supporting Information.
- [24] The relative affinity  $K_{\text{G,DMF}}$  corresponds to the equilibrium:  $1.\text{Zn}^{2+} + \text{DMF} + \text{G} \rightleftharpoons 1.\text{Zn}^{2+} + \text{G} + \text{DMF}$ .
- [25] S. Le Gac, M. Luhmer, O. Reinaud, I. Jabin, *Tetrahedron* 2007, 63, 10721–10730.
- [26] The corresponding experiments were carried out in  $\text{CDCl}_3$ , a medium sufficiently similar to  $\text{CD}_2\text{Cl}_2$ , to be able to conclude with confidence on the validity of these results in  $\text{CD}_2\text{Cl}_2$ .
- [27] The calculated energy of the first intermediate (+24 kJ/mol) is probably lower as it is heavily impacted by the solvation energy of a free water



- molecule (-21 kJ/mol), which we believe is largely overestimated in our model.
- [28] G. Izzet, M.-N. Rager, O. Reinaud, *Dalton Trans.* **2007**, 771–780.
- [29] L. Helm, A. E. Merbach, *Coord. Chem. Rev.* **1999**, 187, 151–181.
- [30] O. Sénèque, M.-N. Rager, M. Giorgi, T. Prangé, A. Tomas, O. Reinaud, *J. Am. Chem. Soc.* **2005**, 127, 14833–14840.
- [31] B. V. Plapp, B. Raj Savarimuthu, D. J. Ferraro, J. K. Rubach, E. N. Brown, S. Ramaswamy *Biochem.* **2017**, 56, 3632–3646.
- [32] P. C. Sanghani, W. I. Davis, L. Zhai, H. Robinson, *Biochem.* **2006**, 45, 4819–4830.
- [33] Y. Sato, H. Hoshino, N. Iki, *J. Inorg. Biochem.* **2016**, 161, 122–127.
- [34] L. C. Costello, C. C. Fenselau, R. B. Franklin, *J. Inorg. Biochem.* **2011**, 105, 589–599.
- [35] W. Maret, Y. Li, *Chem. Rev.* **2009**, 109, 4682–4707.
- [36] a) A. D. Becke, *Phys. Rev. A* **1988**, 38, 3098–3100; b) J. P. Perdew, *Phys. Rev. B* **1986**, 33, 8822–8824.
- [37] a) S. Grimme, S. Ehrlich, L. Goerigk, *J. Comput. Chem.* **2011**, 32, 1456–1465; b) S. Grimme, J. Antony, S. Ehrlich, H. Krieg, *J. Chem. Phys.* **2010**, 132, 154104.
- [38] a) F. Neese, *Wiley Interdiscip. Rev.: Comput. Mol. Sci.* **2012**, 2, 73–78; b) F. Neese, *Wiley Interdiscip. Rev.: Comput. Mol. Sci.* **2017**, 8, e1327.
- [39] F. Weigend, R. Ahlrichs, *Phys. Chem. Chem. Phys.* **2005**, 7, 3297–3305.
- [40] A. V. Marenich, C. J. Cramer, D. G. Truhlar, *J. Phys. Chem. B* **2009**, 113, 6378–6396.

---

Manuscript received: June 18, 2021

Accepted manuscript online: July 21, 2021

Version of record online: August 11, 2021